

Selective Run-Length Encoding

Xutan Peng, Yi Zhang, Dejia Peng, and Jiafa Zhu

Huawei Galois Lab

{pengxutan, zhangyi418, pengdejia, zhujiafa}@huawei.com

Abstract

Run-Length Encoding (RLE) is one of the most fundamental tools in data compression. However, its compression power drops significantly if there lacks consecutive elements in the sequence. In extreme cases, the output of the encoder may require more space than the input (aka *size inflation*). To alleviate this issue, using combinatorics, we quantify RLE’s space savings for a given input distribution. With this insight, we develop the first algorithm that *automatically* identifies suitable symbols, then selectively encodes these symbols with RLE while directly storing the others without RLE. Through experiments on real-world datasets of various modalities, we empirically validate that our method, which maintains RLE’s efficiency advantage, can effectively mitigate the size inflation dilemma.

1 Introduction

Run-Length Encoding (RLE) is a simple yet powerful data compression technique that can be used to losslessly encode *runs*, i.e., sequences of repeated symbols, in a compact form [1]. The basic idea behind RLE is to represent each element only once, followed by its count within the run. For instance, $\langle \mathbf{a}, \mathbf{b}, \mathbf{b}, \mathbf{b}, \mathbf{a}, \mathbf{a}, \mathbf{c}, \mathbf{c}, \dots \rangle$ can be stored as $\langle \mathbf{a}, \mathbf{b}, \mathbf{a}, \mathbf{c}, \dots \rangle$ (namely an *encoded variable*) together with $\langle \mathbf{1}, \mathbf{3}, \mathbf{2}, \mathbf{2}, \dots \rangle$ (namely a *run-control variable*). Note that the encoded variable and the run-control variable are equal in length. Binary code for an element in the run-control variable is usually implemented with a fixed width (denoted as b_r) and can thus represent a run length $\in [1, 2^{b_r}]$. Should the length (denoted as n) exceed 2^{b_r} , this run will be separated into $\lceil \frac{n}{2^{b_r}} \rceil$ divisions by RLE to avoid overflow [2, 3].

RLE can significantly reduce the size of the encoded data, especially when dealing with repetitive patterns or long sequences. In addition, it is easy to implement and incurs a low overhead (with the time complexity being $\mathcal{O}(N)$ during both encoding and decoding). As a result, RLE becomes one of the most important compressors in applications where speed and simplicity are key factors: Digital Archive [4], Time-Series Database [5], and Image Codec (e.g., BMP and JPEG [6]), to list a few.

Nevertheless, the *vanilla* RLE has its Achilles’ heel: if long runs are missing in the input sequence, the output may occupy even more space [7]. One straightforward solution is to perform two RLE passes. The first pass is *exploratory* and involves all symbols. It identifies symbols *suitable* to RLE, i.e., symbols whose total size in the output (encoded variable and run-control variable) is no larger than the input, in a post-hoc fashion. The second pass, which acts as the actual compression, only

We would like to express our sincerest gratitude to Liwei Guo, Zhaoyi Sun, Fang Li, Jie Liu, Guanyi Chen, Yi Xin, Ruizhe Li, and Shuwei Qian for their insightful and helpful comments.

encodes symbols discovered in the first pass (i.e. suitable to RLE) and leaves other symbols unaffected. The major downside of this method is the computation cost. In particular, when there are various binary representation options (e.g., § 4.1), finding the best configuration, undesirably, requires multiple exploratory RLE passes.

Another popular workaround tackles this efficiency drawback via a heuristic: symbols with higher frequencies are more likely to be suitable to RLE. Therefore, it obtains the input distribution (with at most one pass) and only handles frequent symbol(s) with RLE [3, 4, 8]. However, determining the *frequency threshold* entirely depends on intuitions and human experience, which is not robust and often leads to size inflation. On one hand, if this threshold is too high and some common symbols are not encoded with RLE, the compression effect can be worse than the vanilla RLE. On the other hand, if RLE handles some relatively rare symbols, the compression performance may again get unideal, e.g., in the worst-case scenarios where all symbols have low frequency, even the most dominant symbol may not be suitable to RLE.

In this paper, we theoretically show that, for an arbitrary symbol, its suitability to RLE can be elegantly determined by joining its frequency and bit width (see Eq. (5); for the sake of brevity, we assume in our derivation that the input symbols are Independently and Identically Distributed (i.i.d.)). Based on this insight, we propose a novel method that *automatically* calculates the aforementioned frequency threshold, and only the symbols that meet this threshold are encoded with RLE. To the best of our knowledge, no one before us has made such an exploration. Next, on both i.i.d. and non-i.i.d. testbeds that cover different real-world modalities (tabular data, time-series, and image), we empirically validate that our algorithm, which retains the efficiency advantage, substantially outperforms existing RLE baselines and consistently avoid the size inflation issue.

2 Preliminaries

Problem formulation. Let N be the length of the input sequence and N_x be the amount of elements whose symbol is x . To decide whether symbol x is suitable to RLE, we need to predict whether these N_x elements require no extra bits in the RLE output compared with those in the input.

To begin with, let $N_x - \mathbb{R}_x$ denote symbol x 's number of occurrences in the encoded variable. As the amount of the corresponding elements in the run-control variable is also $N_x - \mathbb{R}_x$ (see § 1), encoding x with RLE saves

$$b_x N_x - (b_x + b_r)(N_x - \mathbb{R}_x) \tag{1}$$

bits in total, where b_x stands for the number of bits used to represent the symbol x . It is clear that to decide whether Eq. (1) ≥ 0 holds, the key task is to compute \mathbb{R}_x .

Calculating \mathbb{R}_x . Following previous data compression works [9–11], we assume that the input sequence is generated from an i.i.d. source. When N is sufficiently large, the probability that symbol x occurs can be written as $p_x = \frac{N_x}{N}$. We can thus estimate the count of runs whose symbols are all x and length is *exactly* n :

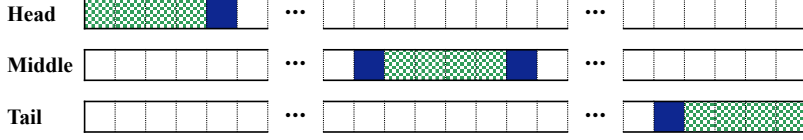


Figure 1: Three possible locations of a run where all symbols are x and the length is precisely $n \leq N - 2$ (in this example $n = 4$). A green (dotted hatch) cell stands for a symbol x , while blue (solid hatch) cells denote other symbols.

- When $n \leq N - 2$, such a run may appear at three different types of locations in the input sequence (see Fig. 1). In the “middle” case, such a run has $N - n - 1$ possible starting indexes. For each index, its occurrence probability is $(1 - p_x)p_x^n(1 - p_x)$. Hence, the expected number of occurrence is $(1 - p_x)p_x^n(1 - p_x)(N - n - 1)$. Similarly, the expected number of such a run’s occurrence is $p_x^n(1 - p_x)$ in the “head” case and $(1 - p_x)p_x^n$ in the “tail” case.
- When $n = N - 1$, such a run may only appear at the sequence’s “head” or “tail”.
- When $n = N$, trivially the number of occurrences is p_x^N .

It is known that encoding a run with a length of exactly n requires $\lceil \frac{n}{2^{b_r}} \rceil$ run-control variable elements (see § 1). Accordingly, we can show that

$$\begin{aligned}
\mathbb{R}_x &= \underbrace{\sum_{n=1}^{N-2} \left(\overbrace{(1 - p_x)p_x^n(1 - p_x)(N - 1 - n)}^{\text{“middle”}} + \overbrace{p_x^n(1 - p_x)}^{\text{“head”}} + \overbrace{(1 - p_x)p_x^n}^{\text{“tail”}} \right) \left(n - \lceil \frac{n}{2^{b_r}} \rceil \right)}_{n \leq N-2} \\
&\quad + \underbrace{\left(p_x^{N-1}(1 - p_x) + (1 - p_x)p_x^{N-1} \right) \left(N - 1 - \lceil \frac{N-1}{2^{b_r}} \rceil \right)}_{n=N-1 \text{ (only “head” and “tail”)}} + \underbrace{p_x^N \left(N - \lceil \frac{N}{2^{b_r}} \rceil \right)}_{n=N} \\
&= p_x^N \left(N - \lceil \frac{N}{2^{b_r}} \rceil \right) + \sum_{n=1}^{N-1} \left(2(1 - p_x)p_x^n + (1 - p_x)^2 p_x^n (N - 1 - n) \right) \left(n - \lceil \frac{n}{2^{b_r}} \rceil \right)
\end{aligned}$$

For clarity, we rewrite this equation as

$$\mathbb{R}_x = \sum_{n=1}^{N-1} (k_\alpha n + k_\beta) p_x^n (n - 1) + \epsilon_1 + \epsilon_2 \quad (2)$$

where $k_\alpha = -(1 - p_x)^2$, $k_\beta = (1 - p_x)((1 - p_x)(N - 1) + 2)$, $\epsilon_1 = p_x^N (N - \lceil \frac{N}{2^{b_r}} \rceil)$, and $\epsilon_2 = \sum_{n=1}^{N-1} (k_\alpha n + k_\beta) p_x^n (1 - \lceil \frac{n}{2^{b_r}} \rceil)$.

If $p_x = 1$, i.e., all input symbols are x , when $N \gg 2^{b_r}$ (which holds in practice), via Eq. (2) trivially we have

$$\mathbb{R}_x = N - \lceil \frac{N}{2^{b_r}} \rceil = \left(1 - \frac{1}{2^{b_r}} \right) N$$

In this case, x is suitable to RLE as long as

$$\text{Eq. (1)} \geq 0 \iff b_x N \geq (b_x + b_r) \left(N - \left(1 - \frac{1}{2^{b_r}} \right) N \right) \iff b_x \geq \frac{b_r}{2^{b_r} - 1} \quad (3)$$

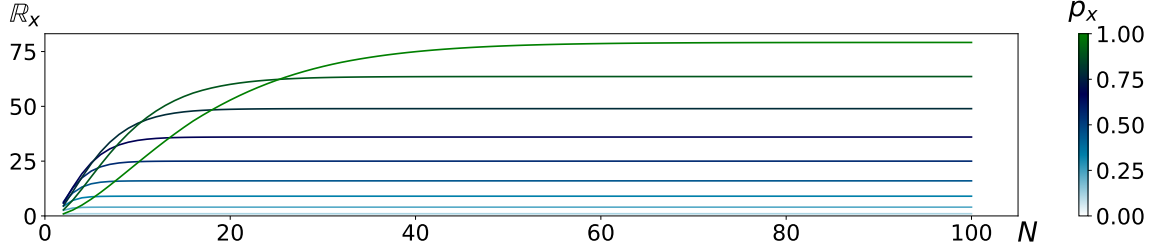


Figure 2: The relationship between \mathbb{R}_x and N , with b_r fixed at 4.

In practice, $b_r \geq 1$, so $1 \geq \frac{b_r}{2^{b_r}-1}$; also $b_x \geq 1$, thus Eq. (3) constantly holds. As a result, if all input elements are the same, RLE is always a suitable compressor.

Otherwise, i.e., $p_x \in (0, 1)$, although we can still exploit Eq. (2) directly to calculate \mathbb{R}_x , the computation overhead is too much. Concretely speaking, via Stirling's formula [12] we know that the time complexity of $\sum_{n=1}^{N-1} (\cdot)^n$ is at least $\mathcal{O}(N \log N)$.

In Fig. 2, we notice that when N surpasses 80, \mathbb{R}_x displays a pronounced tendency towards convergence. In practice, N is typically orders of magnitude larger than 80. Therefore, we can simplify the calculation of \mathbb{R}_x by solving its limit. To be detailed, we first transform the summation of finite series to that of finite series as

$$\begin{aligned} \mathbb{R}_x &= \sum_{n=1}^{\infty} (k_\alpha n + k_\beta) p_x^n (n-1) + \epsilon_1 + \epsilon_2 + \epsilon_3 \\ &= k_\alpha \sum_{n=1}^{\infty} p_x^n n^2 + (k_\beta - k_\alpha) \sum_{n=1}^{\infty} p_x^n n - k_\beta \sum_{n=1}^{\infty} p_x^n + \epsilon_1 + \epsilon_2 + \epsilon_3 \end{aligned}$$

where $\epsilon_3 = -\sum_{n=N}^{\infty} (k_\alpha n + k_\beta) p_x^n (n-1)$. Then, using the three lemmas justified in the Appendix, we can show that

$$\begin{aligned} \mathbb{R}_x &= k_\alpha \left(\frac{p_x^2 + p_x}{(1-p_x)^3} - 0 \right) + (k_\beta - k_\alpha) \left(\frac{p_x}{(1-p_x)^2} - 0 \right) - k_\beta \left(\frac{1}{1-p_x} - 1 \right) + \epsilon_1 + \epsilon_2 + \epsilon_3 \\ &= p_x^2 (N-1) + \epsilon_1 + \epsilon_2 + \epsilon_3 \end{aligned}$$

Approximation analysis. We show that ϵ_1 can be neglected when N is sufficiently large and $p_x \in (0, 1)$. Given $f(x) = \frac{\ln x}{x}$ is monotonically increasing, we have

$$\frac{\ln(p_x N)}{p_x N} < \frac{\ln(N)}{N} \iff N \ln(p_x N) < (p_x N) \ln N \iff (p_x N)^N < N^{p_x N}$$

Because $N - p_x N = N - N_x \geq 1$,

$$\epsilon_1 = p_x^N \left(N - \left\lceil \frac{N}{2^{b_r}} \right\rceil \right) < p_x^N N = \frac{(p_x N)^N}{N^{p_x N}} \cdot \frac{N}{N^{N-p_x N}} < \frac{N}{N^{N-p_x N}} \leq 1 \ll N$$

As for ϵ_2 and ϵ_3 , combining them yields

$$\epsilon_2 + \epsilon_3 = \sum_{n=1}^{\infty} (k_\alpha n + k_\beta) p_x^n - \left[\sum_{n=1}^{N-1} (k_\alpha n + k_\beta) p_x^n \left\lceil \frac{N}{2^{b_r}} \right\rceil + \sum_{n=N}^{\infty} (k_\alpha n + k_\beta) p_x^n n \right] \quad (4)$$

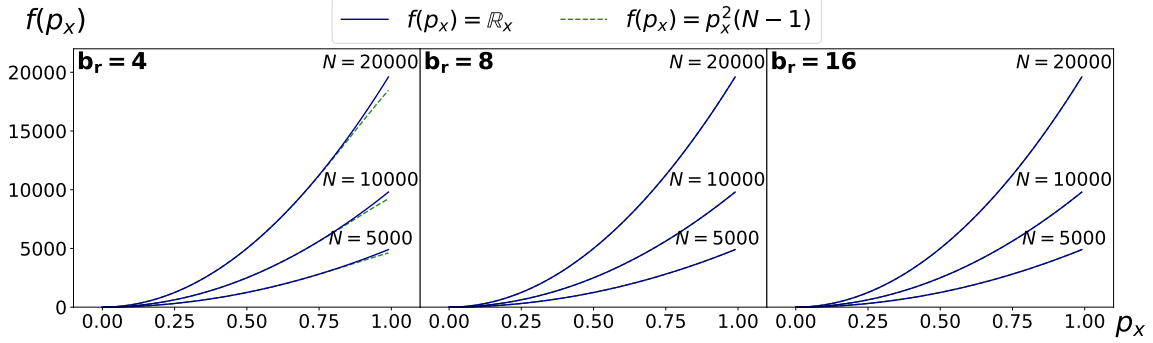


Figure 3: Comparisons between \mathbb{R}_x and $p_x^2(N-1)$ under different configurations.

Instead of quantifying the complex Eq. (4), we investigate its impact by directly plotting \mathbb{R}_x and $p_x^2(N-1)$ for comparison. As shown in Fig. 3, in settings with various b_r and N , \mathbb{R}_x and $p_x^2(N-1)$ almost coincide perfectly when $b_r \geq 8$. In the case that $b_r = 4$, their trends still match well, especially when $p_x \leq 0.75$. As for $p_x > 0.75$, i.e., most input symbols are x , it is almost certain that RLE serves as a suitable compressor for x and solving Eq. (1) is no longer necessary. We thus argue that the minor difference between \mathbb{R}_x and $p_x^2(N-1)$ is negligible in practice. Moreover, based on the observation that $\mathbb{R}_x \gtrsim p_x^2(N-1)$, we have

$$p_x^2(b_x + b_r)(N-1) \geq N_x \cdot b_r \implies (b_x + b_r)\mathbb{R}_x \geq b_r N_x \implies \text{Eq. (1)} \geq 0$$

i.e., in terms of guaranteeing that encoding x with RLE will not lead to more considerable storage usage, substituting \mathbb{R}_x with $p_x^2(N-1)$ in Eq. (1) will never lead to incorrect decisions. What is even better, this approximation can significantly reduce the time complexity of the computing \mathbb{R}_x from $\mathcal{O}(N \log N)$ to $\mathcal{O}(1)$.

Finally, when $p_x \in (0, 1)$, the threshold of identifying x as a symbol that RLE may encode can be derived as

$$\begin{aligned} p_x^2(b_x + b_r)(N-1) \geq b_r N_x &\iff (b_x + b_r)(N-1)\left(\frac{N_x}{N}\right)^2 \geq b_r N_x \\ &\iff N_x \geq \frac{b_r}{b_x + b_r} \cdot \frac{N^2}{N-1} \end{aligned}$$

which, given N is sufficiently large in practice, can be simplified as

$$N_x \geq \frac{b_r}{b_x + b_r} \cdot N \iff p_x \geq \frac{b_r}{b_x + b_r} \quad (5)$$

Remarkably, since Eq. (5) always holds when $N_x = N$, it also works when $p_x = 1$.

3 Algorithm

Compression. In § 2, we identified the criterion to assess the suitability of applying RLE on specific symbols. Based on this, we propose compressing only a subset of the input sequence while leaving other symbols unaffected. To be exact,

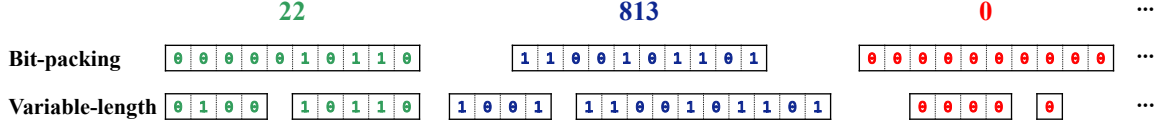


Figure 4: Examples of the two binary representation schemes we consider in § 4.1 (all elements are less than 2^{10}). NB: for each variable-length code, the components on the left and right are c_α and c_β , respectively.

- **Step 1: Constructing set \mathcal{G} .** We add x to \mathcal{G} (a set) if Eq. (5) holds, so that \mathcal{G} contains all symbols suitable to RLE. In case the symbols' frequencies are unknown, we randomly sample elements from the input to infer the distribution.
- **Step 2: Encoding.** Scanning the entire input sequence, if the occurred symbol can be found in \mathcal{G} , our algorithm will store it in the encoded variable and the count of its consecutive repeats in the run-control variable, i.e., identical to how the vanilla RLE behaves. Otherwise, our approach will directly append this symbol to the encoded variable, regardless of its successor. For instance, with $\mathcal{G} = \{\mathbf{a}, \mathbf{b}\}$, $\langle \mathbf{a}, \mathbf{b}, \mathbf{b}, \mathbf{b}, \mathbf{a}, \mathbf{a}, \mathbf{c}, \mathbf{c}, \dots \rangle$ (the same example sequence in § 1) will be rendered as $\langle \mathbf{a}, \mathbf{b}, \mathbf{a}, \mathbf{c}, \mathbf{c}, \dots \rangle$ and $\langle 1, 3, 2, \dots \rangle$.

Decompression. Our algorithm scans the encoded variable. If a symbol belonging to \mathcal{G} occurs, it will be repeated for r times in the reconstructed sequence, where r denotes the first *unvisited* element in the run-control variable. Otherwise, this symbol will be directly appended to the reconstructed sequence without repetition.

Discussion. As \mathcal{G} only contains sufficiently frequent symbols, its cardinality (which is normally below a dozen in practice), as well as size, can be neglected. Therefore, as long as the input sequence satisfies the i.i.d. assumption, our scheme can lead to no worse compression than the vanilla RLE. More importantly, in theory, the output of our algorithm is guaranteed to be no larger in size than the input.

In practice, increasing the sample size at the compression stage may lead to a better estimation on the distribution of the entire input sequence, while consuming more computational resources. When the sequence is long and segmentation is needed before compression, sampling should be done on each segment. In any case, obtaining the input distribution needs at most one full pass, so the time complexity of constructing \mathcal{G} is $\mathcal{O}(N)$. Because the encoding process also takes $\mathcal{O}(N)$, the overall compression time complexity is still $\mathcal{O}(N)$. Similarly, the decompression time complexity is $\mathcal{O}(N)$. To sum up, our algorithm substantially enhances the compression performance of the vanilla RLE, with the efficiency advantage retained.

4 Experiments

4.1 Setups

Implementation details. The lower b_r is, the more likely Eq. (5) holds, i.e., the stronger RLE's compression power on x tends to be. Therefore, by default, we set b_r at 4, the minimum configuration widely used in literature [2, 6, 13]. When dealing

with each input sequence, we randomly sample 10K elements to generate \mathcal{G} . As for the binary representation of symbols, we consider two widely adopted strategies, as illustrated in Fig. 4:

- **Bit-packing** [14]: Each symbol is represented by b bits, with b being the minimum number of bits required to encode any symbol.
- **Variable-length** [15]: Each symbol is encoded into two components, namely c_α and c_β . c_α stores the width of c_β (empirically we fix the width of c_α at 4 bits). c_β represents the symbol’s actual value, using the fewest number of bits necessary.

Testbeds. We utilise the following resources, which cover three distinct modalities:

- **SO-2018**¹ stores the responses in a survey conducted in 2018 by Stack Overflow, a famous online developer community. This tabular archive contains answers to 128 queries (such as personal background, skill set, and job preferences) in the questionnaire, which are processed as 128 input sequences in our experiment. Since the 0.1 million rows (each corresponds to one respondent) have been randomly permuted for anonymisation purposes, this dataset can be regarded as a prime example of (approximately) i.i.d. sequences in the real world.
- **Netstream** is a private dataset held by Huawei. It comprises traffic monitoring logs collected via our internal telecommunication devices. We focus on 5 landmark entries, each of which includes over 17 million records. Please be aware that this large-scale time-series dataset does not satisfy the i.i.d. assumption.
- **“Lena”**² is the premier standard test image in the field of data compression. To flatten it, for simplicity, we adopt a workflow motivated by the compression procedure of the BMP format [6]. To be concrete, we first convert the original image to a bitmap and then concatenate all pixel lines. As a result, “Lena” (originally boasts a resolution of 512×512) is transformed into a sequence with 262,144 elements.

Remarkably, many symbols in SO-2018 and Netstream are long strings. Following [7, 8, 11], within every sequence, we replace each symbol with an integer identifier based on its order of appearance (starting from 0 and incremented cumulatively).

Studied methods. Besides the proposed algorithm (abbreviated as **Ours**), we additionally benchmark two baselines: **V-RLE** (aka the vanilla RLE), which handles all symbols with RLE; **D-RLE**, which only encodes the most dominant symbol with RLE (mentioned in § 1; it can be regarded as a special case of **Ours**, where \mathcal{G} always has the most dominant symbol as its only item).

4.2 Results

SO-2018. To provide clear and unified results on all the 128 columns and both binary representation settings, as demonstrated in Fig. 5, we report the Compression Ratio (CR), i.e., $\frac{\text{input size}}{\text{output size}}$ (the higher, the better). Overall, we observe that despite achieving successful compression sometimes (see data points on the right of each sub-figure), V-RLE struggles on most columns. This is because most columns of SO-2018 have high cardinality, where even the most dominant value has a low frequency.

¹<https://insights.stackoverflow.com/survey/2018>

²http://www.lenna.org/lena_std.tif

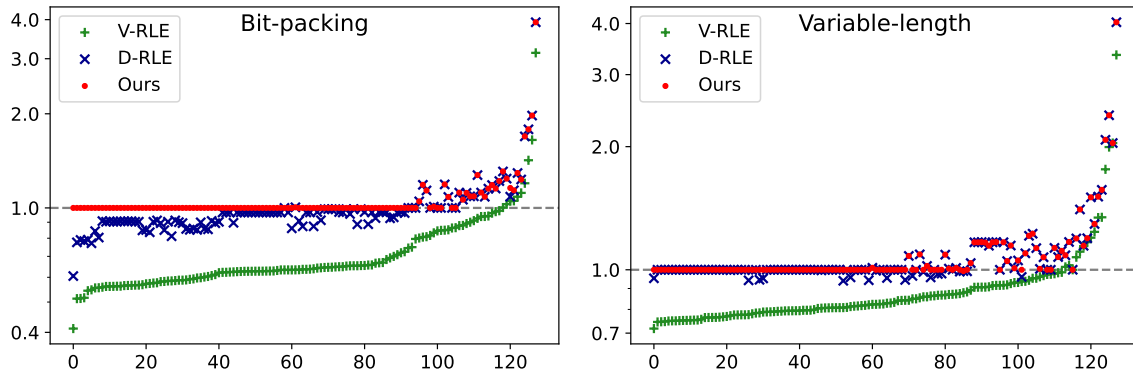


Figure 5: Column-wise log-scaled Compression Ratio (CR, the higher the better) on the SO-2018 dataset. Data points with the same X coordinate correspond to the same column (for visibility, the 128 columns are sorted according to the CR of V-RLE).

	Bit-packing						Variable-length					
	V-RLE		D-RLE		Ours		V-RLE		D-RLE		Ours	
Src_IP	409.5	[-68.3]	364.6	[-23.4]	341.2	[0.0]	426.5	[-41.7]	423.8	[-39.0]	384.8	[0.0]
Dst_IP	334.9	[-10.1]	308.4	[16.4]	303.5	[21.3]	428.5	[-76.5]	421.6	[-69.6]	352.0	[0.0]
Src_Port	282.3	[-9.3]	280.6	[-7.6]	273.0	[0.0]	315.4	[-25.9]	304.2	[-14.7]	289.5	[0.0]
Dst_Port	227.0	[-36.0]	205.8	[-14.8]	191.0	[0.0]	216.2	[14.6]	213.6	[17.2]	198.0	[32.8]
Protocol	66.2	[10.1]	65.5	[10.8]	63.2	[13.1]	68.0	[3.3]	61.6	[6.4]	60.7	[7.3]

Table 1: Entry-wise size (MB) of Netstream after encoding. In both this table and Tab. 2, we highlight the smallest size of each setting in **bold**, and additionally calculate the *reduced* size (see the square bracket on the right of every cell).

Implied from § 2, under such a distribution, the number of occurrences of long runs is low, and V-RLE is thus unsuitable. As for the existing workaround, D-RLE, it does address this challenge to some degree: on most columns, it yields higher CR than V-RLE. Nevertheless, we still see many columns where the output of D-RLE is undesirably larger than the input in size. In contrast, the CR of Ours is not only on par with or above that of either counterpart on *all* columns, but also *always* equal to or higher than 1.0. In other words, our experiments confirm that Ours, which substantially outperforms V-RLE and D-RLE, consistently avoids the size inflation issue when the i.i.d. assumption is (approximately) satisfied.

Netstream. Although in § 2 we assume the input to be i.i.d., on non-i.i.d. data such as Netstream, we still find our method effective. As displayed in Tab. 1, Ours consistently compresses the time-series to the smallest size. Also, it is the only approach that never requires more bits for the output than the input. In comparison, on all the 10 examined settings, V-RLE and D-RLE end up with negative storage space reduction for 7 and 6 times, respectively.

“Lena”. We exploit three popular bitmap palette configurations, which respectively require 4, 8, and 16 bits (aka *colour depth*) for each pixel, so as to support 16, 256, and 65,536 colours. Following the BMP standard [6], we fix the binary representation at bit-packing, and consider $b_r \in \{4, 8\}$ with $b_r \leq b_x$ for RLE. Results in Tab. 2


	# of colours	b_x (colour depth)	b_r	V-RLE		D-RLE		Ours	
	16	4	4	238.1	[-110.1]	135.2	[-7.2]	128.0	[0.0]
	16	8	4	363.4	[-107.4]	257.3	[-1.3]	256.0	[0.0]
	256	8	8	484.5	[-228.5]	258.8	[-2.8]	256.0	[0.0]
	65,536	16	4	635.8	[-123.8]	512.1	[-0.1]	512.0	[0.0]
	65,536	16	8	762.9	[-250.9]	512.2	[-0.2]	512.0	[0.0]

Table 2: Size (KB) of “Lena” after encoding.

re-verify the superiority of **Ours** when compressing non-i.i.d. input. To be concrete, **V-RLE** increases the storage space in all setups by large margins. While this problem tends to be less severe on **D-RLE**, we still observe size inflation, especially on smaller b_x . **Ours**, on the contrary, identifies no suitable symbol for \mathcal{G} , so that RLE is not actually applied. Therefore, although **Ours** yields zero compression effect on “Lena”, it guarantees that the size does not explode, which is critical in practice.

5 Conclusion and Future Work

This paper concerns the long-standing size inflation challenge of RLE. We first derive an elegant equation to automatically identify symbols suitable to RLE, based on which we develop an algorithm that selectively handles part of the input sequence with RLE. Next, on real-world tabular, time-series, and image testbeds, we empirically validate that (1) the proposed method constantly avoids size inflation, and (2) it is substantially superior to existing RLE techniques.

While our experimental results on non-i.i.d. datasets are promising, the theoretical analysis presented in § 2 is restricted to the i.i.d. context. In the future, we will extend our theory to more complex distributions, as well as testify the proposed algorithm on more diverse applications.

References

- [1] Solomon W. Golomb, “Run-length encodings (Corresp.),” *IEEE Transactions on Information Theory*, vol. 12, pp. 399–401, 1966.
- [2] Shmuel T. Klein and Dana Shapira, “Practical fixed length Lempel-Ziv coding,” *Discrete Applied Mathematics*, vol. 163, pp. 326–333, 2014, Stringology Algorithms.
- [3] Myeongjae Jang, Jinkwon Kim, Haejin Nam, and Soontae Kim, “Zero and narrow-width value-aware compression for quantized convolutional neural networks,” *IEEE Transactions on Computers*, 2023.
- [4] Sven Fiergolla and Petra Wolf, “Improving run length encoding by preprocessing,” in *2021 Data Compression Conference (DCC)*. IEEE, 2021, pp. 341–341.
- [5] Davis W. Blalock, Samuel Madden, and John V. Guttag, “Sprintz: Time series compression for the internet of things,” in *ACM on Interactive, Mobile, Wearable and Ubiquitous Technologies (IMWUT)*, 2018.
- [6] John Miano, *Compressed image file formats - JPEG, PNG, GIF, XBM, BMP*, Addison-Wesley-Longman, 1999.
- [7] Khalid Sayood, *Introduction to data compression*, Morgan Kaufmann, 1996.
- [8] Dirk Gandolph, Jobst Hörentrup, Axel Kochale, Ralf Ostermann, and Hartmut Peters, “Method for run-length encoding of a bitmap data stream,” 2010, US Patent 7,657,109.

- [9] Kar-Ming Cheung and Aaron B. Kiely, “An efficient variable length coding scheme for an IID source,” in *Data Compression Conference (DCC)*, 1995.
- [10] Mark Z. Mao, Robert M. Gray, and Tamás Linder, “On asymptotically optimal stationary source codes for IID sources,” in *Data Compression Conference (DCC)*, 2011.
- [11] Daniel Severo, James Townsend, Ashish Khisti, Alireza Makhzani, and Karen Ullrich, “Compressing multisets with large alphabets,” *IEEE Journal on Selected Areas in Information Theory*, 2023.
- [12] Philippe Flajolet and Robert Sedgewick, *Analytic Combinatorics*, Cambridge University Press, 2009.
- [13] Kenny Daily, Paul Rigor, Scott Christley, Xiaohui Xie, and Pierre Baldi, “Data structures and compression algorithms for high-throughput sequencing technologies,” *BMC Bioinformatics*, vol. 11, pp. 1–12, 2010.
- [14] Hao Jiang, Chunwei Liu, John Paparrizos, Andrew A Chien, Jihong Ma, and Aaron J Elmore, “Good to the last bit: Data-driven encoding with CodecDB,” in *International Conference on Management of Data (SIGMOD)*, 2021.
- [15] Latha Pillai, “Variable length coding,” *Application Note: Virtex-II Series*, 2003.

Appendix

Lemma 1.

$$\sum_{n=0}^{\infty} a^n = \frac{1}{1-a} \quad \text{subject to} \quad a \in (0, 1)$$

Proof. By summing up a Geometric Progression and finding its limit, for $a \in (0, 1)$, we can show that

$$\sum_{n=0}^N a^n = \frac{a^0(1-a^{N+1})}{1-a} \implies \sum_{n=0}^{\infty} a^n = \lim_{N \rightarrow \infty} \frac{a^0(1-a^{N+1})}{1-a} = \frac{1}{1-a} \quad \square$$

Lemma 2.

$$\sum_{n=0}^{\infty} a^n n = \frac{a}{(1-a)^2} \quad \text{subject to} \quad a \in (0, 1)$$

Proof. It can be justified by respectively calculating the derivatives of both sides of the equation in Lemma 1, as

$$\frac{d}{da} \sum_{n=0}^{\infty} a^n = \frac{d}{da} \frac{1}{1-a} \iff \sum_{n=0}^{\infty} a^{n-1} n = \frac{1}{(1-a)^2} \iff \sum_{n=1}^{\infty} a^n n = \frac{a}{(1-a)^2} \quad \square$$

Lemma 3.

$$\sum_{n=0}^{\infty} a^n n^2 = \frac{a^2 + a}{(1-a)^3} \quad \text{subject to} \quad a \in (0, 1)$$

Proof. Similar to the previous proof, we simply differentiate both sides of the equation in Lemma 2, yielding

$$\begin{aligned} \frac{d}{da} \sum_{n=0}^{\infty} a^n n &= \frac{d}{da} \frac{a}{(1-a)^2} \iff \sum_{n=0}^{\infty} a^{n-1} n^2 = \frac{(1-a)^2 + 2a(1-a)}{(1-a)^4} = \frac{a+1}{(1-a)^3} \\ &\iff \sum_{n=0}^{\infty} a^n n^2 = \frac{a^2 + a}{(1-a)^3} \quad \square \end{aligned}$$